

Electronic Supporting Information

Autonomous reaction self-optimization using in-line high-field NMR spectroscopy

Nour El Sabbagh,^a Margherita Bazzoni,^a Yuliia Horbenko,^a Aurélie Bernard,^a Daniel Cortés-Borda,^a Patrick Giraudeau,^a François-Xavier Felpin,^{*a} Jean-Nicolas Dumez^{*a}

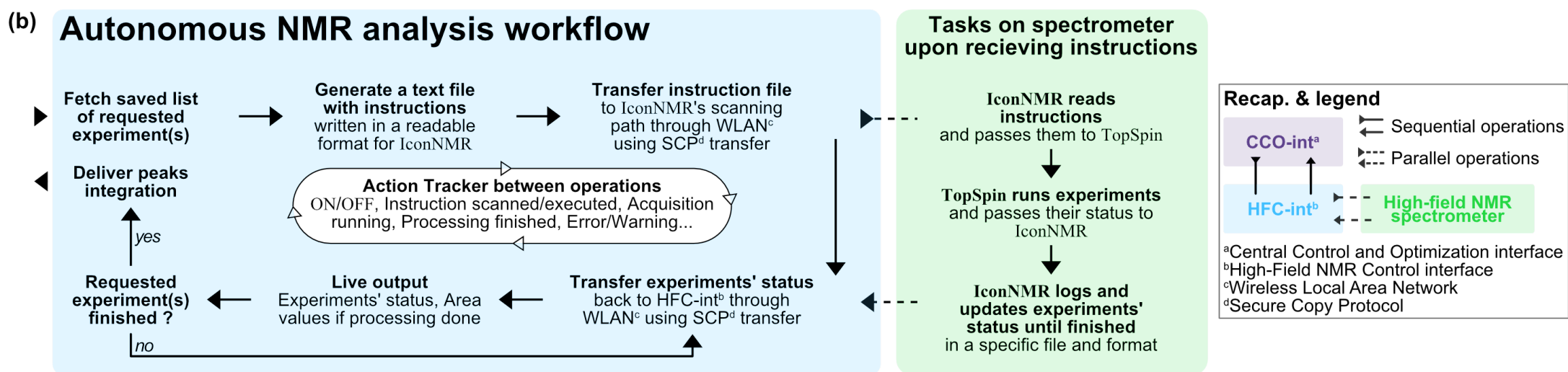
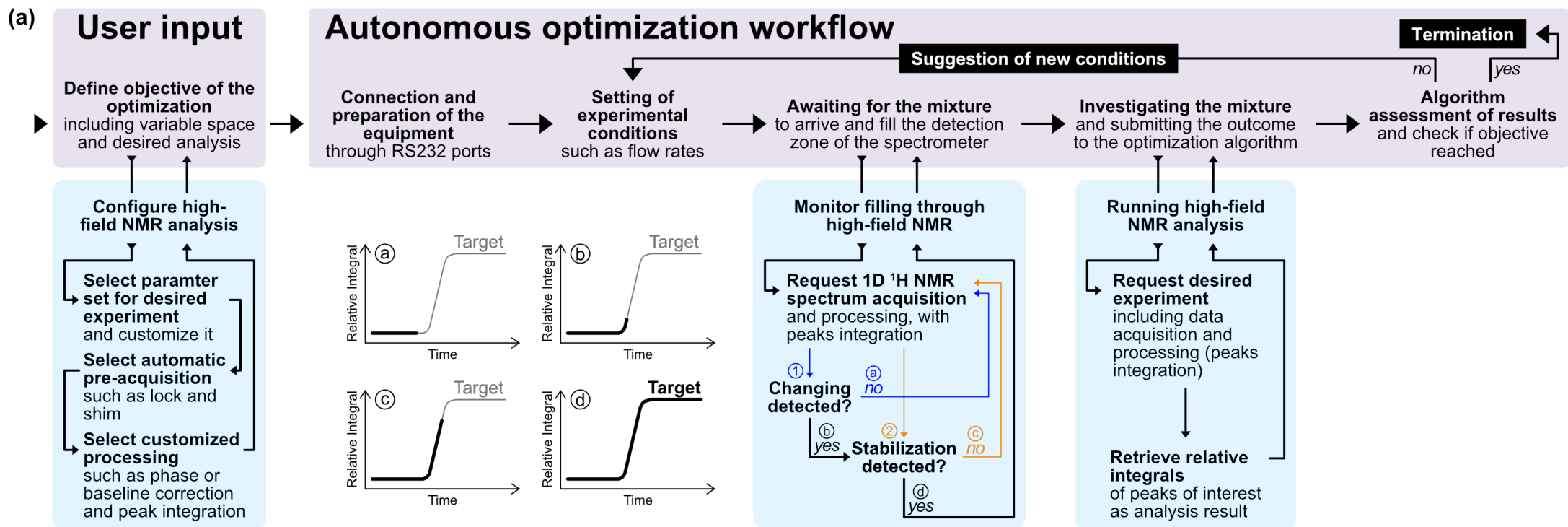
^aNantes Université, CNRS, CEISAM UMR 6230, F-44000 Nantes (France).

E-mail : Francois-Xavier.Felpin@univ-nantes.fr ; Jean-Nicolas.Dumez@univ-nantes.fr

Table of contents

1. Supplementary scheme	3
2. Supplementary figures	4
3. Supplementary tables	14
4. Supplementary equations	16

1. Supplementary scheme



Scheme S1. Diagram detailing the autonomous workflow of both interfaces, CCO-int (a) and HFC-int (b). The communication between both interfaces is presented, as well as the parallel automated workflow of IconNMR and TopSpin on the spectrometer's computer.

2. Supplementary figures

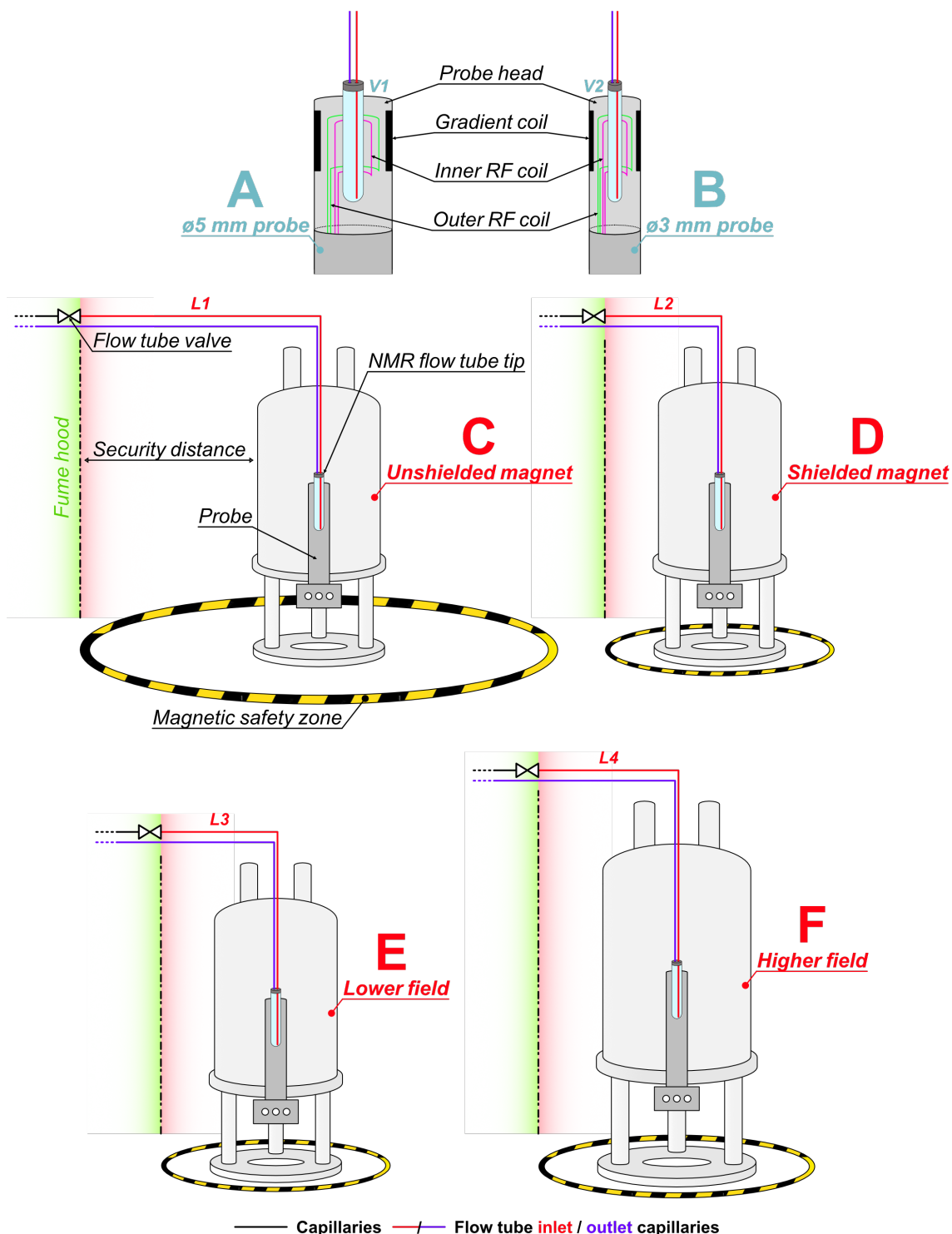


Figure S1. Representation of how the total volume of the flow unit is modified according to the NMR equipment used. This volume is directly related to the flow line inlet length (L) and the NMR tube tip size (V). If the NMR tube tip were to be changed, e.g., when using another probe head with a smaller sample diameter (from A to B), the volume of the NMR tube tip will decrease ($V_2 < V_1$). This leads to a smaller volume of mixture required to completely flush and fill it and reach a steady state regime, as the volume of the pumped mixture depends on the geometry of the flow tube tip. On the other hand, switching from an unshielded magnet to a shielded one (from C to D) significantly reduces the required flow line length ($L_2 < L_1$), while increasing the magnetic field intensity (from E to F) may extend it ($L_4 > L_3$). The direct consequence of modifying this length is the minimum volume of the flow reactor, in such setup where the transport line of the flow tube tip is part of it.

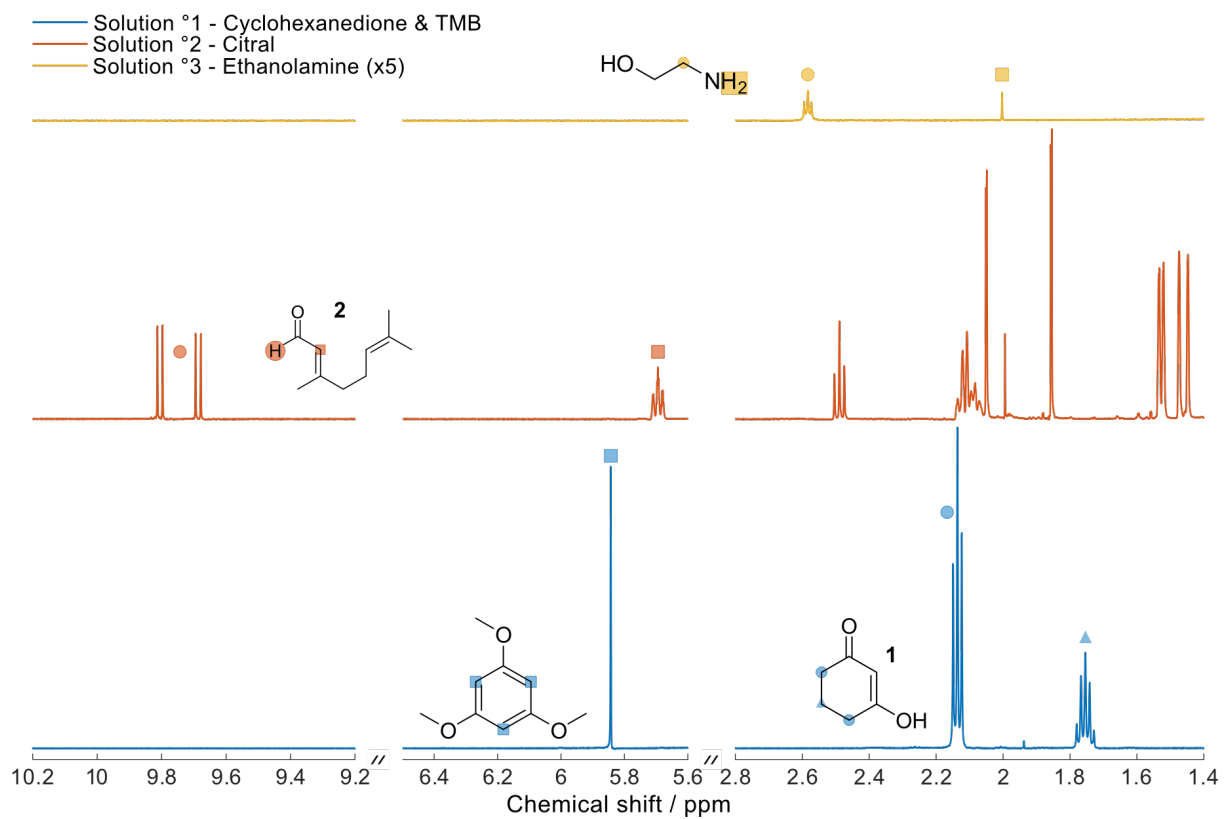


Figure S2. 1D ^1H spectra acquired of the prepared solutions using 5 mm NMR tubes. Regions presenting solvent suppression artefacts were cut off from each spectrum.

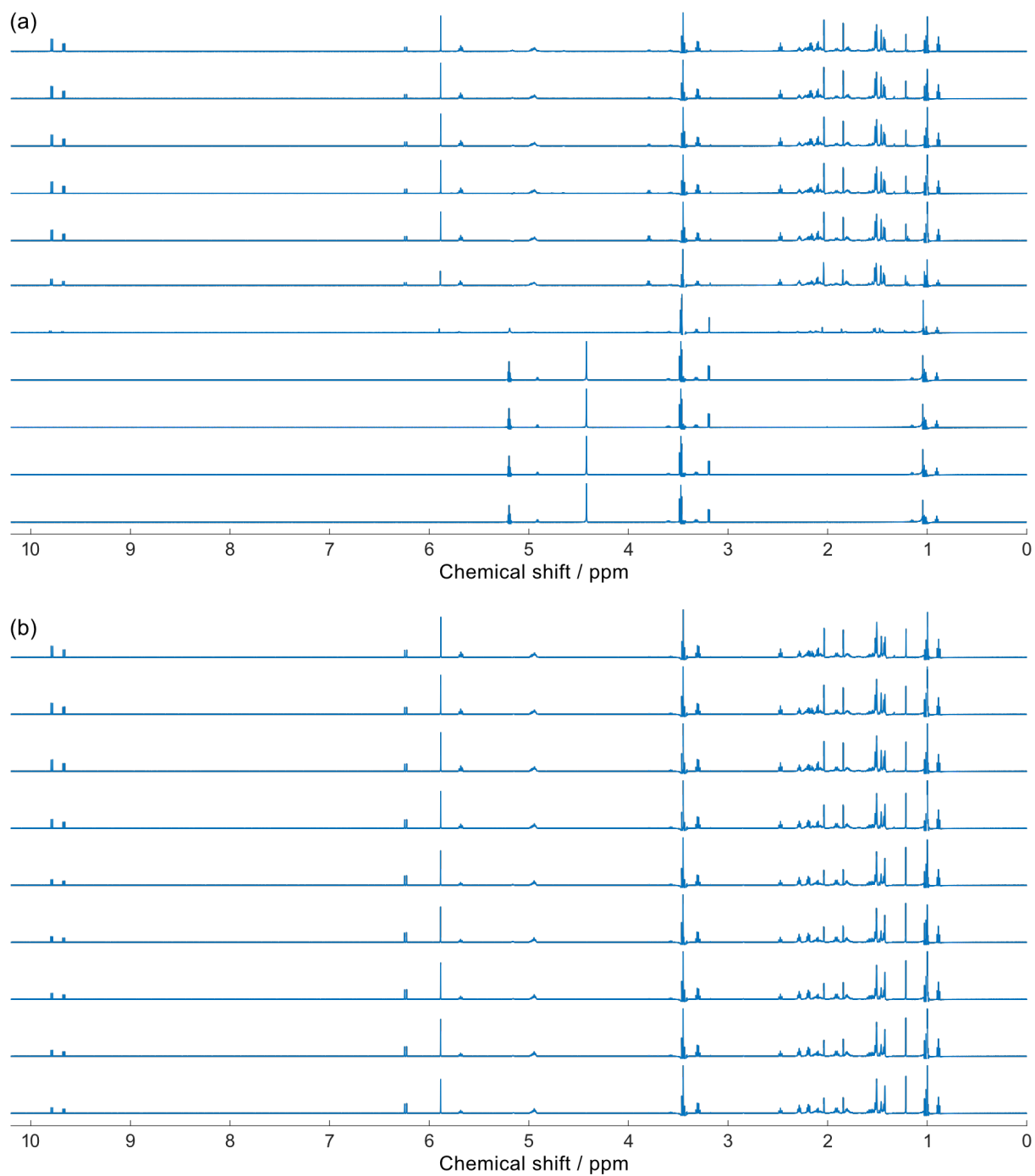


Figure S3. Continuous 1D ^1H spectra acquired during two examples of reaction mixtures filling the NMR tube tip during two different reaction runs: (a) a major change of state during the filling and (b) a minor change of state. Data were acquired in flow, following the launch of the reaction run, to monitor the arrival of the mixture of interest in the NMR detection zone. Here, a shimming procedure was applied before the first two data acquisitions and then alternated after every two consecutive ones.

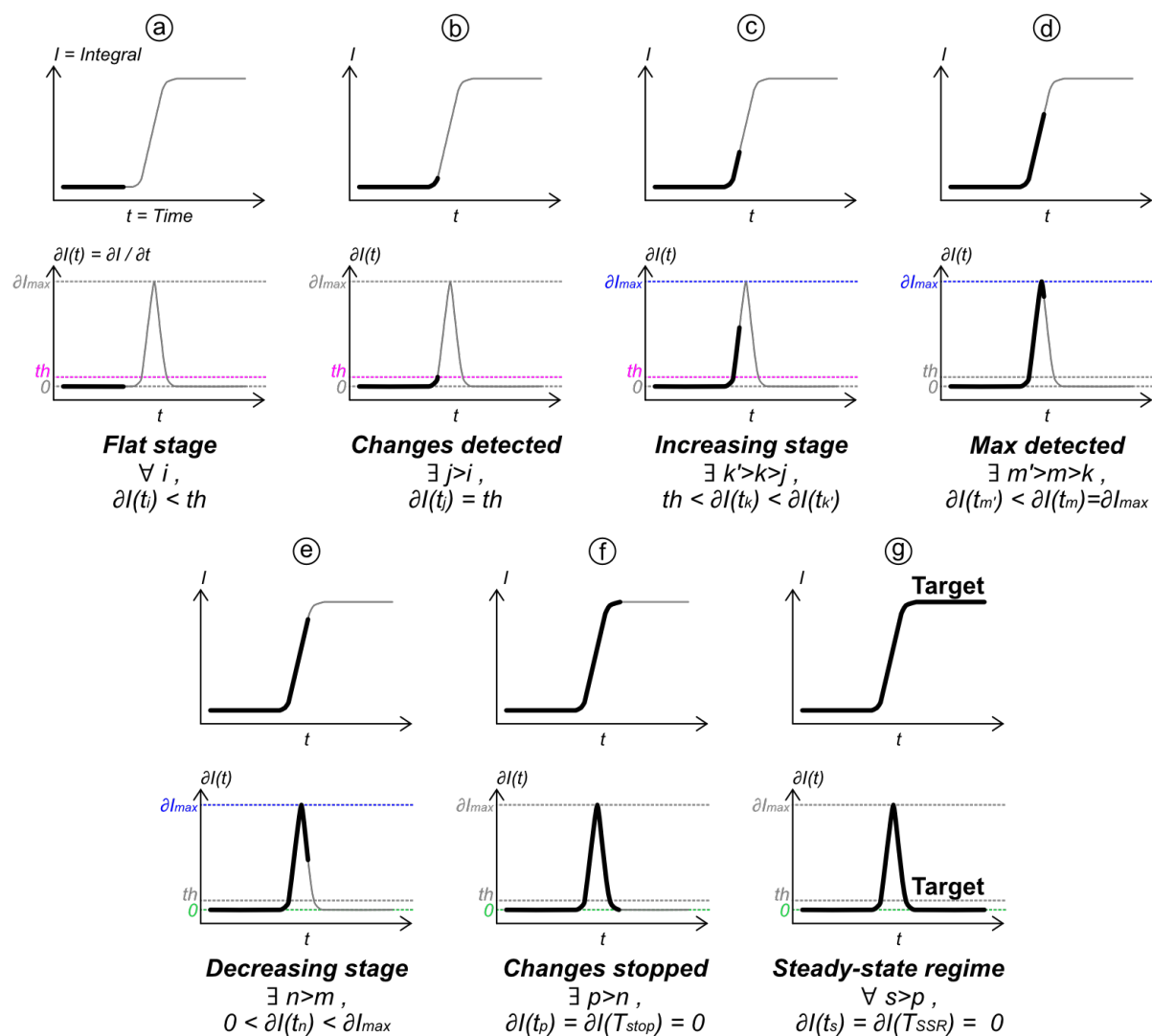


Figure S4. Illustration of how different stages can be detected through NMR analysis during an experiment conducted using our experimental flow setup. Continuous acquisition of 1D ^1H NMR and integration of peaks of interest I within the spectra are performed during the monitoring. Experiment stages can be distinguished while monitoring the derivative of the integrals ∂I in function of time t , which demonstrates any changes occurring to I . (a) Upon launching an experiment, the new reaction mixture formed starts travelling through the flow reactor before reaching the NMR detection zone. No changes detected yet at the NMR level, and ∂I remains equal to zero. A threshold is set, as integrals in real experimental data might oscillates while performing acquisition on flow. (b, c) Once the new mixture arrives at the NMR detection zone, integrals start varying furthermore, which is notably portrayed by the derivative function. Here, ∂I exceeds the threshold set and continuously increases. The new mixture start filling the NMR detection zone. (d) At the middle of the rise of the integrals, the derivative function reaches a peak, manifesting a maximum changing rate. (e, f) As the integrals keep increasing, the changing rate slows down where ∂I starts decreasing. Here, the filling of the NMR detection zone with the new mixture is almost done. At a time T_{stop} , ∂I reaches a zero value, which indicates that the integrals have just stopped changing. (g) As back mixing phenomena can highly occur when flowing chemicals, it is always better to avoid performing the desired NMR analysis of the new mixture at T_{stop} and to wait for a stabilization. The latter can be customized, as the stabilization stage totally depends on how much one could allow spending extra volume of reaction mixture in order to ensure reaching a steady-state regime (SSR). TSSR is the time required to safely reach the SSR. For a given flow rate FR , the required volume V_{SSR} can be determined as $V_{SSR} = FR * T_{SSR}$, which should be consistent for the same experimental setup. Subsequently, instead of continue monitoring the SSR for each experiment, the system can simply calculate the time required to reach it according to the employed flow rate and the required volume previously determined, as $T_{SSR}(i) = V_{SSR} / FR(i)$.

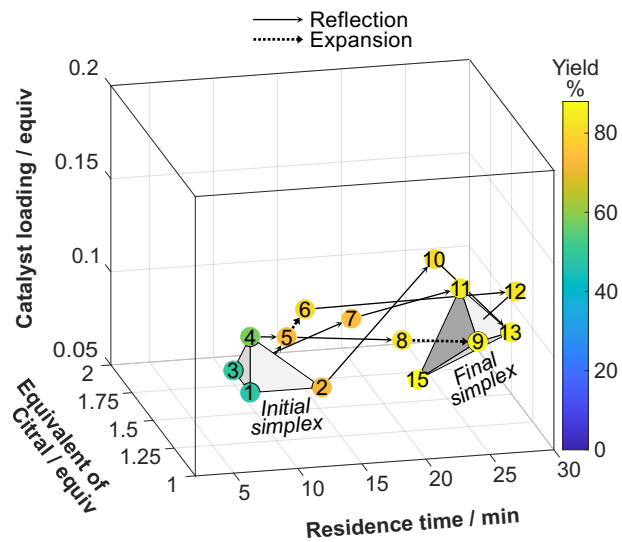


Figure S5. Representation in the variable space of the steps and operations taken by Nelder-Mead algorithm during the yield optimization. Initial and final simplex are also presented.

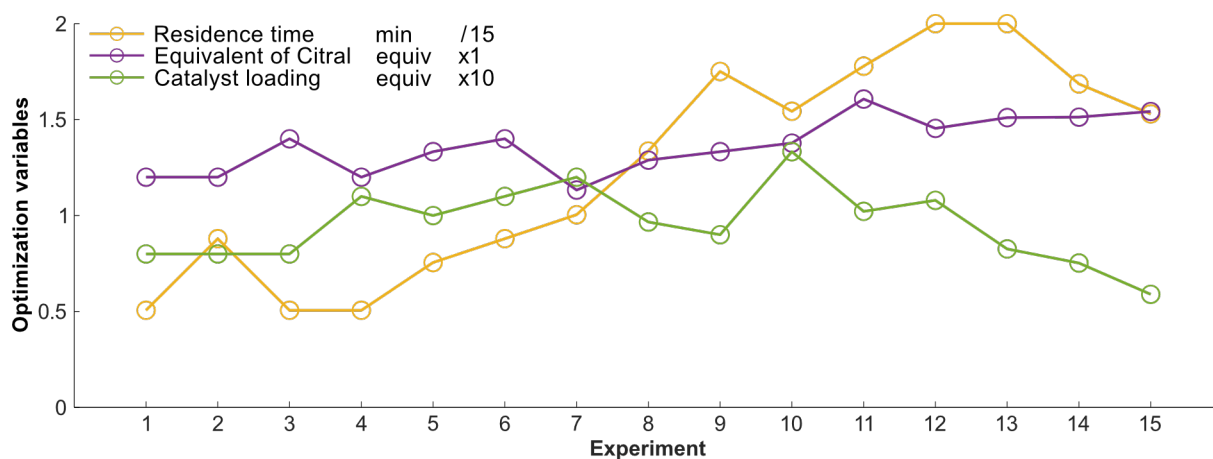


Figure S6. Variations of the reaction parameters during the maximization of the yield of the studied reaction. For a more concise representation on a single graph, the residence time (min) values were normalized by dividing them by 15 and the catalyst loading (equiv) values were amplified by a factor of 10, while the equivalent of citral (equiv) values remained unchanged.

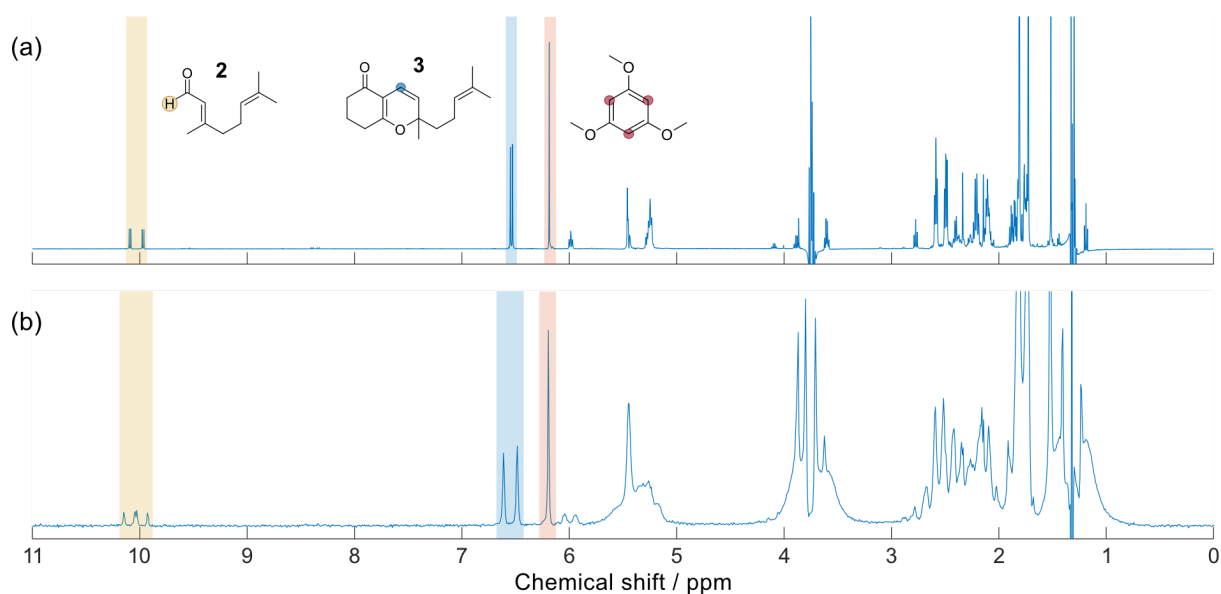
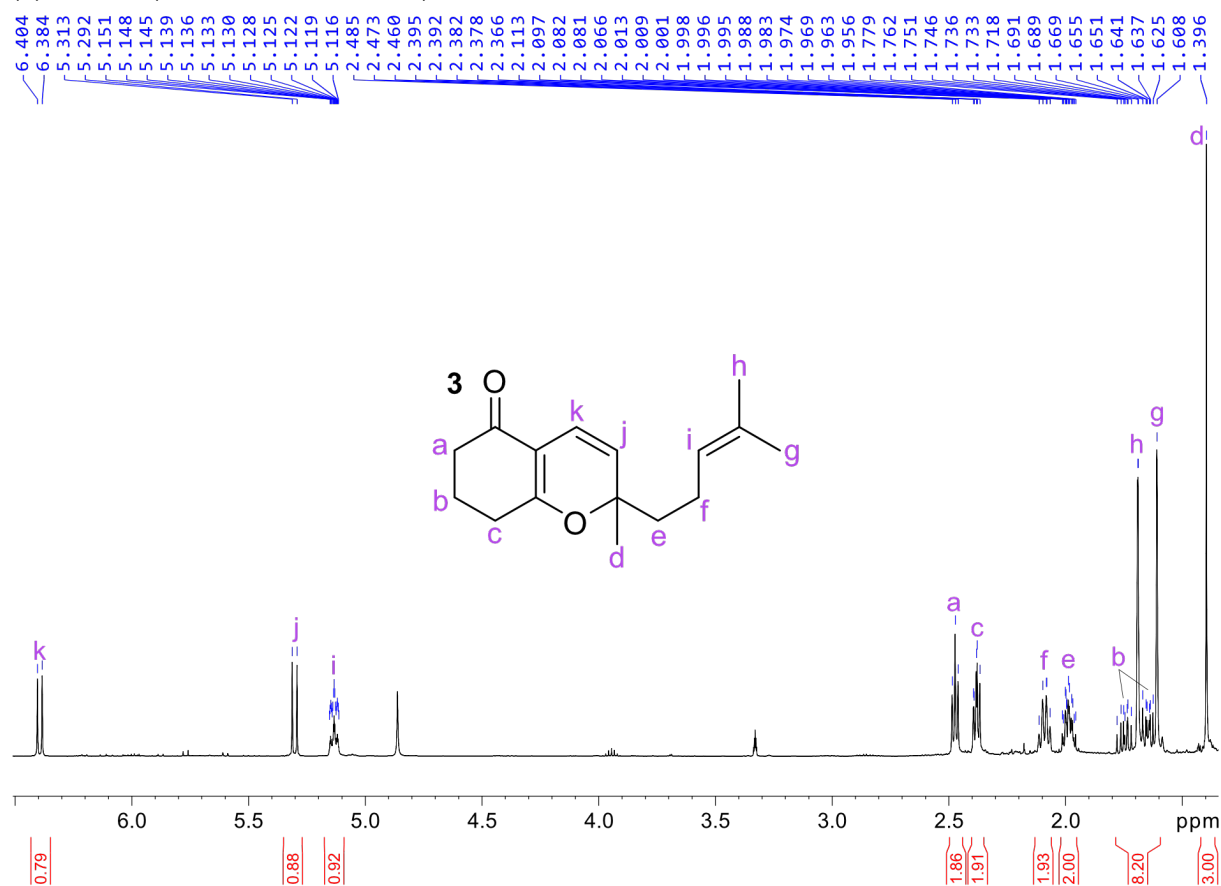


Figure S7. 1D ^1H spectra of the same reaction mixture were acquired at 500.13 MHz (a) and 80.27 MHz (b). Around 1.5 mL of the reaction mixture was prepared by mixing volume ratios 0.27/0.41/0.31 of solutions S1/S2/S3 in order to reproduce, in an NMR tube, experiment n°15 of the yield optimization campaign. 0.6 mL of the prepared mixture was introduced into two NMR tubes. After around 26 min of the mixture preparation, high-field and low-field 1D ^1H NMR spectra were both acquired with 1 scan and recovery delay between two consecutive acquisitions of 10.00 s, but with spectral width of 20 and 10 ppm, acquisition time of 6.71 and 1.64 s and a receiver gain of 32 and 52, for which the total experimental time were 16.71 and 11.64 s, respectively. In both cases, the rectangles highlight the peaks of interest of the produced 2*H*-pyran **3** (blue), the citral **2** (yellow) the internal reference (red).

(a) ^1H NMR (500 MHz, Methanol- d_4)



(b) ^{13}C NMR (125 MHz, Methanol- d_4)

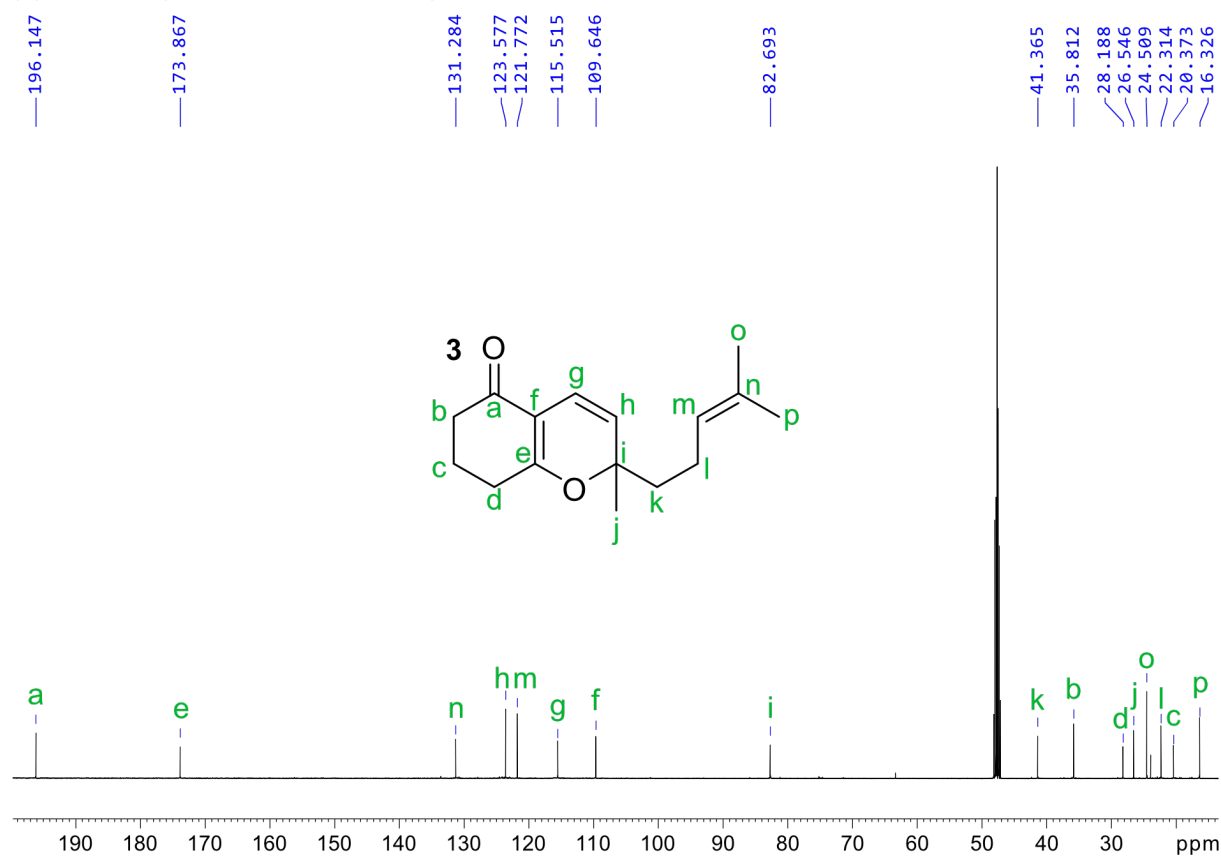


Figure S8. 1D ^1H (a) and ^{13}C (b) NMR spectra were acquired at 500 and 125 MHz, respectively, on a sample of 0.3 M of the purified compound **3** in MeOD.

Throughput maximization

Building on insights gained from the yield optimization, we narrowed down the residence time range from 2-30 min to 10-20 min. The starting point for this variable was set at 12 min, corresponding to the lower bound extended by 20% of the range. The other two dimensions of the variable space remained unchanged and a budget of 15 experiments was set as the termination criterion for this optimization as well.

The results, presented in Figure S6, demonstrated an increase in throughput from approximately 2 mmol/h to 2.6 mmol/h. Table S2 provides details on each experiment, and Figure S7 shows the evolution of the optimized variables. Once again, residence time played a significant role in the optimization goal, but this time, shorter residence times contributed to higher throughput. This second optimization campaign lasted for 5 hours and 20 minutes, and as with yield optimization, we terminated the optimization process after 15 experiments.

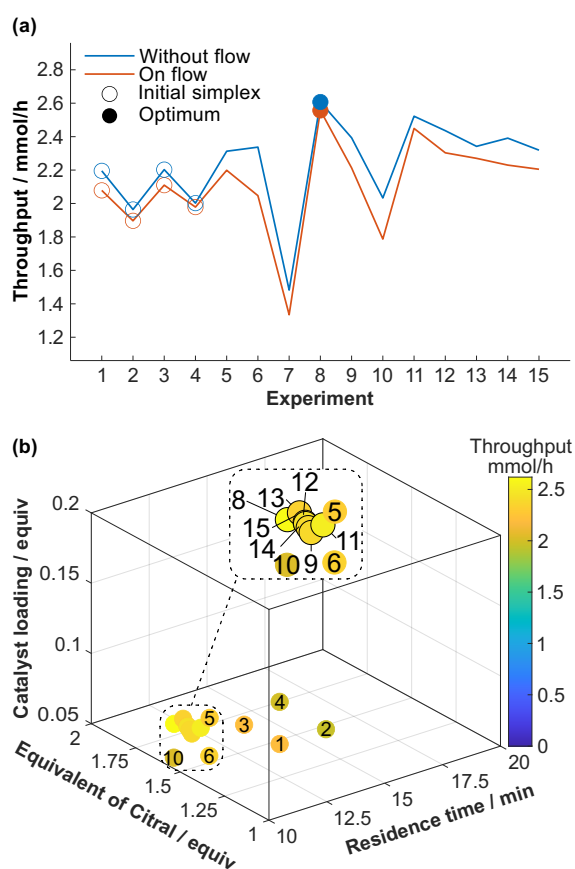


Figure S9. (a) Throughput evolution during the second optimization using our autonomous optimization platform. Results for both on and without flow analyses are shown, as well as the initial simplex and optimum. (b) Representation of the throughput optimization in the 3-dimensional variable space. Each dot represents a set of reaction parameters, where its colour reflects the throughput, determined from the NMR analysis without flow of the corresponding reaction run.

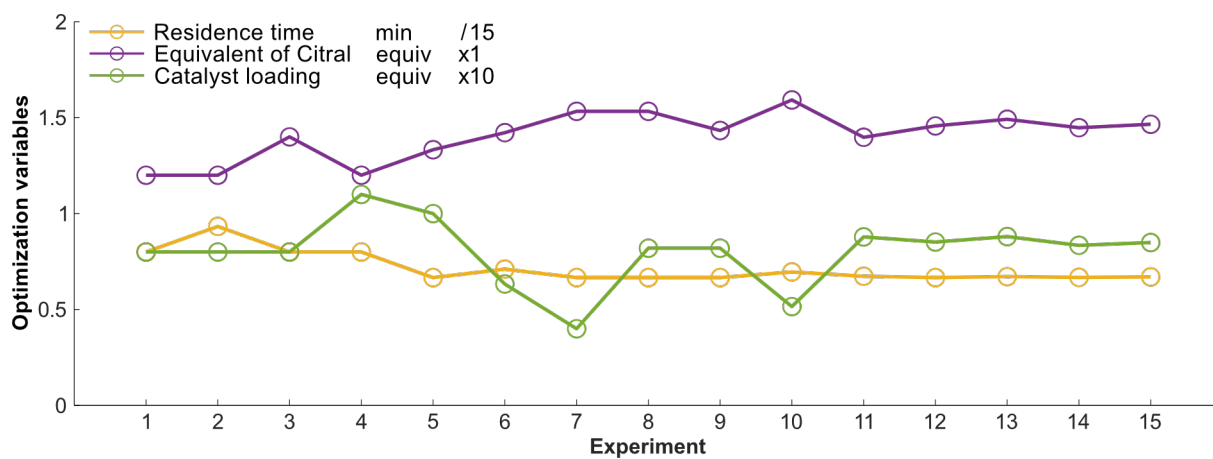


Figure S10. Variations of the reaction parameters during the maximization of the throughput of the studied reaction. For a more concise representation on a single graph, the residence time (min) values were normalized by dividing them by 15 and the catalyst loading (equiv) values were amplified by a factor of 10, while the equivalent of citral (equiv) values remained unchanged.

3. Supplementary tables

Table S1. Maximization of the reaction yield during the first optimization campaign. In blue the experiments corresponding to the 1st simplex, and in orange the ones corresponding to the last simplex.

Run	Residence time (min)	Equiv. of Citral (equiv)	Catalyst loading (equiv)	Yield (%)
1	7.6	1.20	0.08	48
2	13.2	1.20	0.08	73
3	7.6	1.40	0.08	50
4	7.6	1.20	0.11	59
5	11.3	1.33	0.10	74
6	13.2	1.40	0.11	80
7	15.1	1.13	0.12	75
8	20.0	1.29	0.10	83
9	26.3	1.33	0.09	87
10	23.2	1.378	0.13	81
11	26.7	1.61	0.10	84
12	30	1.45	0.11	83
13	30	1.51	0.08	86
14	25.3	1.51	0.08	88
15	23	1.54	0.06	88

Table S2. Maximization of the reaction throughput during the second optimization campaign. In blue the experiments corresponding to the 1st simplex, and in orange the ones corresponding to the last simplex.

Run	Residence time (min)	Equiv. of Citral (equiv)	Catalyst loading (equiv)	Throughput (mmol/h)
1	12	1.20	0.08	2.205
2	14	1.20	0.08	1.972
3	12	1.40	0.08	2.212
4	12	1.20	0.11	2.010
5	10	1.33	0.10	2.323
6	10.7	1.42	0.06	2.348
7	10	1.53	0.04	1.486
8	10	1.53	0.08	2.620
9	10	1.43	0.08	2.404
10	10.4	1.59	0.05	2.041
11	10.1	1.40	0.09	2.534
12	10	1.46	0.09	2.447
13	10.1	1.49	0.09	2.353
14	10	1.45	0.08	2.402
15	10.1	1.47	0.08	2.330

4. Supplementary equations

Yield

The integration of the peak of the produced 2*H*-pyran **3** at 6.13-6.34 ppm (Int_{Prod}) and the one of the internal reference at 5.8-6 ppm (Int_{Ref}) were calculated within the 1D 1H NMR spectra acquired after each experiment. Knowing the number of 1H nuclei describing these peaks ($nbH_{Prod} = 1$, $nbH_{Ref} = 3$) and the concentration ratio α between the limiting reactant **1** ($C_{LimitReact}$) and the internal reference (C_{Ref}) in stock solution S1, the yield can be determined as follow:

$$Yld (\%) = \frac{Int_{Prod}/nbH_{Prod}}{Int_{Ref}/nbH_{Ref} \times \alpha} \times 100,$$

Equation S1

$$\alpha = \frac{C_{LimitReact} (M)}{C_{Ref} (M)}.$$

Throughput

The throughput calculation is derived from the yield as shown below:

$$Th (mol/h) = Yld (\%) \times C'_{LimitReact} (M) \times FR_t (L/h),$$

Equation S2

$$C'_{LimitReact} = C_{LimitReact} \times \frac{FR_1}{FR_t},$$

where FR_1 is the flow rate set on pump 1, pumping stock solution S1, and $C'_{LimitReact}$ and FR_t are the concentration of the limiting reactant **1** and the final flow rate in the flow reactor, respectively.